

IFMIF-EVEDA SC $\beta=0.094$ HALF-WAVE RESONATOR STUDY

E. Zaplatin, Forschungszentrum Juelich, Germany

P. Bosland, Ph. Bredy, N. Grouas, Ph. Hardy, J. Migne, A. Mosnier, F. Orsini, J. Plouin, CEA-Saclay, France

Abstract

The driver of the International Fusion Material Irradiation Facility (IFMIF) consists of two 125 mA, 40 MeV cw deuteron accelerators [1-2]. A superconducting option for the 5 to 40 MeV linac based on Half-Wave Resonators (HWR) has been chosen. The first cryomodule houses 8 HWR's with resonant frequency of 175 MHz and geometric $\beta=v/c=0.094$. This paper describes the RF design of half-wave length resonator together with structural analyses. Detailed simulations of resonance multipactor discharge in HWR are presented. Due to the required high coupling, the power coupler is located in mid-plane of the cavity. Several cavity tuning options were investigated: the capacitive tuner located in mid-plane and opposite to the power coupler port offers a large tuning range and will be tested first.

CAVITY RF DESIGN

The goal of the cavity electro-dynamics design is to optimise the cavity geometry to minimize values of peak electrical and magnetic fields on the cavity surface relative to the accelerating electrical field on the cavity axes (B_{pk}/E_{acc} and E_{pk}/E_{acc}). The fabrication technology and resonator structural properties also should be taken into account from the very beginning of the design. For low-beta cavity design RF parameters do not play the same important role like for elliptical cavities. An enhancement of an accelerating field by 20-30% doesn't result in the substantial reduction of an accelerator length or the number of cavities. That's why the project values for E_{acc} are usually easily achievable. It means, for this type of resonators the stability of the cavity structure against any external distortions is the primer design goal.

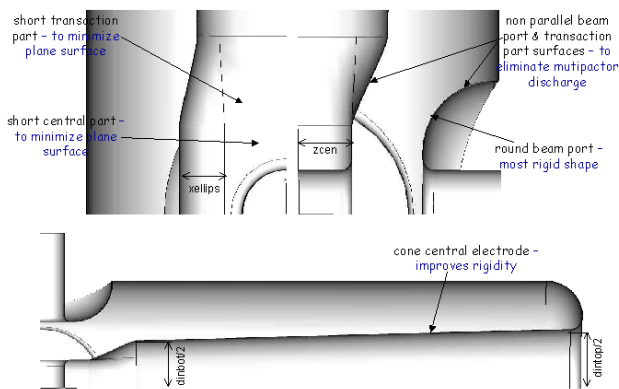


Figure 1: HWR design basics.

Since IFMIF accelerator will work in cw regime, the main goal of our cavity structural design is a minimization of the resonant frequency dependence on

07 Cavity design

the external pressure fluctuations. The general basics of the cavity structural design are to avoid using the plane surfaces. This was the reason of the choice of a round shape of the beam port electrodes (Fig.1). The racetrack shape of the central electrode and the transition part from racetrack to circular part were made as short as possible. Together with the round beam port shape this makes cavity more rigid and allows avoiding the parallel surfaces in the central region to minimize the risk of multipactor.

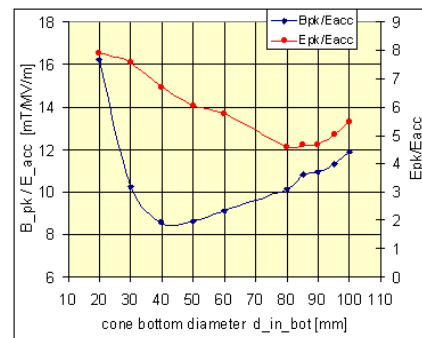


Figure 2: HWR central electrode cone shape optimisation.

To achieve a higher mechanical stability the resonant line of the central electrode was made conical. The conical shape will also reduce the peak magnetic field value. Fig. 2 presents ratios B_{pk}/E_{acc} and E_{pk}/E_{acc} in the process of an optimisation of the lower cone diameter (d_{in_bot} , Fig. 1). There is a clear optimum for B_{pk}/E_{acc} by $d_{in_bot}=42$ mm. Still, this is in contradiction with E_{pk}/E_{acc} optimisation and $d_{in_bot}=80$ mm has been chosen. It allows to reduce E_{pk}/E_{acc} by 50% to compare with $d_{in_bot}=42$ mm whereas B_{pk}/E_{acc} is increased only by less than 20%. For the RF cavity design the whole geometry has been parameterised and all parameters have been optimised. The only given data for the design were the resonant cavity frequency 175 MHz, relative particle speed $\beta=0.094$, the cavity outer conductor diameter 180 mm and a beam pipe aperture radius 20 mm.

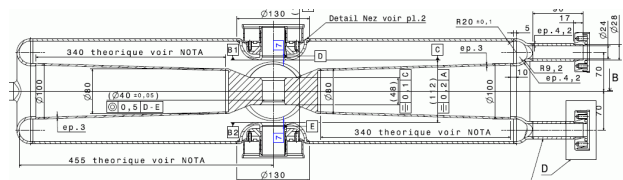


Figure 3: Half-wave resonator drawing and its position in cryomodule.

The cavity geometry is shown in Fig.3 and cavity parameters are summarized in Table 1.

Table 1: Some parameters of half-wave resonator.

Frequency	MHz	175
$\beta=v/c$		0.094
$R_{aperture}$	mm	20
$\beta\lambda$	mm	161.04
R_{cavity}	mm	90
G	Ohm	28.55
$E_{pk} / E_{acc}^*)$		4.42
$B_{pk} / E_{acc}^*)$	mT/MV/m	10.12
$E_{pk} @ E_{acc} = 4.5 \text{ MV/m}$	MV/m	19.87
$B_{pk} @ E_{acc} = 4.5 \text{ MV/m}$	mT	45.56
Cool-down frequency shift	kHz	250
BCP frequency shift	kHz/100 μm	40
df / dp	Hz/mbar	0.04
$K_L = df / (E_{acc})^2$	Hz/(MV/m) ²	1.1
*) $L_{cav} = N_{gaps} * \beta\lambda/2$, where $N_{gaps}=2$ – number of gaps		

MULTIPACTOR SIMULATIONS

Multipacting in rf structures is a resonant process in which a large number of electrons build up an multipacting discharge, absorbing rf power so that it becomes impossible to increase the cavity fields by raising the incident power. An electron can be emitted from one of the structure’s surface by different reasons. The emitted electron is accelerated by the rf fields and eventually impacts a wall again, thereby producing secondary electrons. The number of secondary electrons depends on the surface characteristics and on the impact energy of the primary. In turn, the secondaries are accelerated and, upon impact, produce another generation of electrons. The process then repeats. An electron current increases exponentially if the number of emitted electrons exceeds the number of impacting ones and if the trajectories satisfy specific resonance conditions. Electrons colliding with structure walls, cause a large temperature rise and eventually to the thermal breakdown.

The simulations of multipactor resonance discharge in the cavity have been provided according to the procedure described in [3]. The whole cavity model for these calculations has been prepared in Microwave Studio. In this study the Furman probabilistic model of secondary emission for copper was used with default MWS PS parameters. Usually 30 generations of secondary electrons were tracked and maximum of secondaries per hit was 3.

The particle sources provided the simulations with primary electrons uniformly distributed over source area and uniformly distributed over energy range 5 eV \pm 50%. Number of primary particles per source was from 50 to 20000. MWS PS stores information on emission and collision for every separately defined surface. This data allows calculating integral secondary emission yield defined as $\langle SEY \rangle = (\text{Total Number of Secondaries}) / (\text{Total$

Number of Hits) and evaluate MP probability, its intensity and zones for each separate surface.

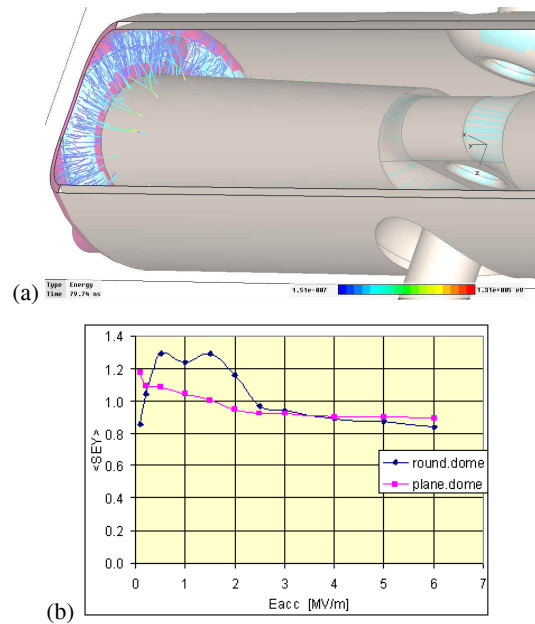


Figure 4: MP study in dome region (a –MP trajectories, b – simulation results).

It is well known that in Half-Wave Resonator the first order multipactor exists in cavity dome volume. Two types of cavity dome shape have been investigated – the round and plane.

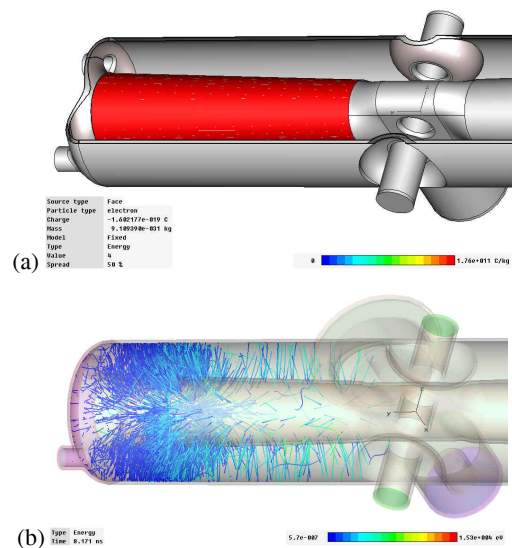


Figure 5: MP study in central cone electrode region (a – geometry with source area, b – MP trajectories).

The trajectories for round dome and simulation results for both dome shapes are presented on Fig.4. The results for plane dome shape detect less chance for MP to compare with round dome (Fig.4b). Still, the round dome shape is preferable for cavity cleaning to simplify the cleaning fluids to withdraw through the dome ports.

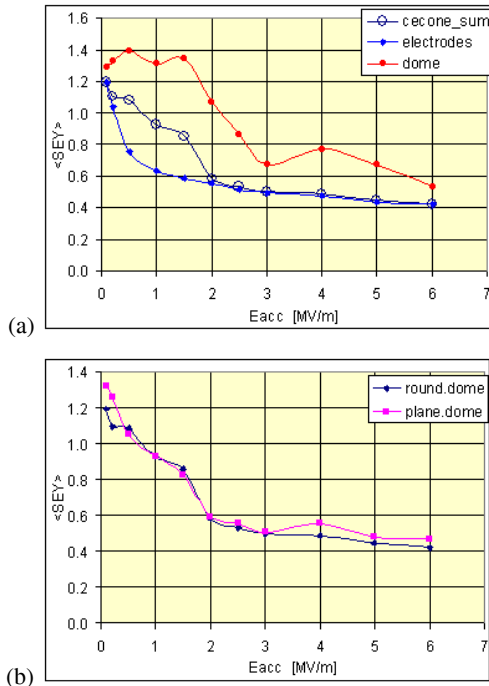


Figure 6: MP study in central cone electrode region (a – simulation results, b – round and plane dome shape comparison).

HWR central electrode together with outer conductor represents a coaxial line that usually affected by MP (Fig.5).

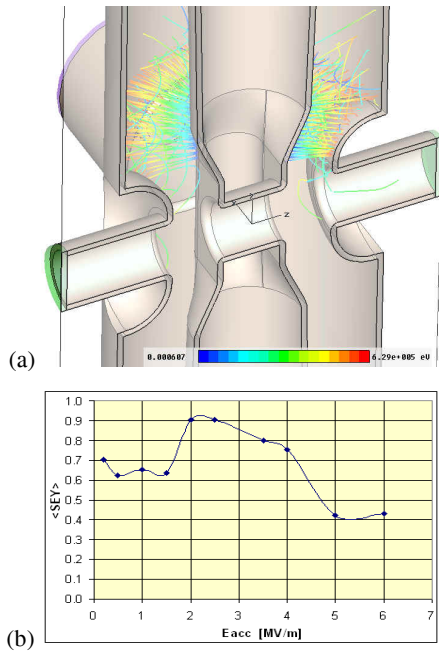


Figure 7: MP study in central region (a – MP trajectories, b – simulation results).

The detailed study of multipactor on different surfaces with central electrode as a primary particle source revealed that the main MP happens in the dome region and only weak low energy MP levels detected between

central electrode and outer conductor (Fig.6a). The comparison of round and plane dome shapes didn't detect any difference in MP levels (Fig. 6b).

One more dangerous zone for MP in HWR is the volume between beam ports and central electrode (Fig.7a). To eliminate MP in this area the surfaces from the beginning were designed nonparallel. The calculations didn't reveal any levels of discharge in this area (Fig.7b).

The power coupler is installed in the cavity central region opposite to the tuner. The position of the coupler tip is 32 mm from the outer cavity conductor inside the coupler resonant line for required $Q_{ext}=5.7 \cdot 10^4$ (Fig.8). The coupler line wave impedance is 50 Ohm with the coupler outer conductor diameter 100 mm.

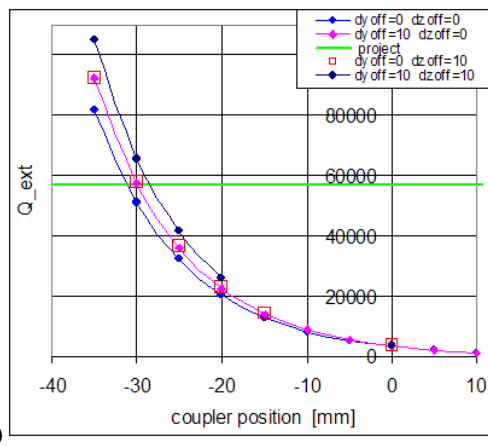
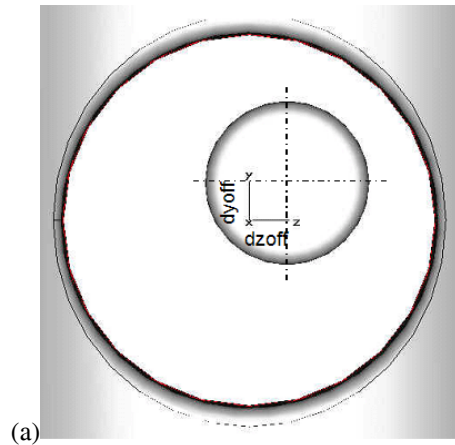


Figure 8: Cavity external quality factor vs. coupler tip position.

The tolerances of coupler central electrode installation have been calculated. Two extreme off-axis offsets of 10 mm of the central electrode in the coupler outer conductor have been investigated (Fig.8a). There is nearly no difference in the results has been detected if central electrode is shifted along only one certain axis – Y or Z. In these cases Q_{ext} is increased by approximately 6500, which is equivalent to 1.5 mm coupler central electrode tip shift. If coupler CE is shifted for 10 mm along both (Y and Z) axes, Q_{ext} enhancement nearly doubles. This would

be equivalent about 2.5-3 mm coupler central electrode tip shift.

STRUCTURAL ANALYSIS

Static External Pressure

The structural analysis of the cavity behaviour under external pressure has been provided. A sequential coupled field analysis RF/Structural/RF is used to predict the frequency drift due to cavity deformations using codes ANSYS. The same meshed model was used for all types of simulations. Such procedure allows getting the highest simulation accuracy [4].

Since the cavity stiffening environment is uncertain at the moment of cavity design, it is worth to provide this study under two cavity beam port constrain conditions – fully fixed and completely free. Fig.9 presents HWR wall deformations and frequency dependency on external pressure fluctuation df/dp with different cavity wall thickness for these two extreme cases of beam port stiffening.

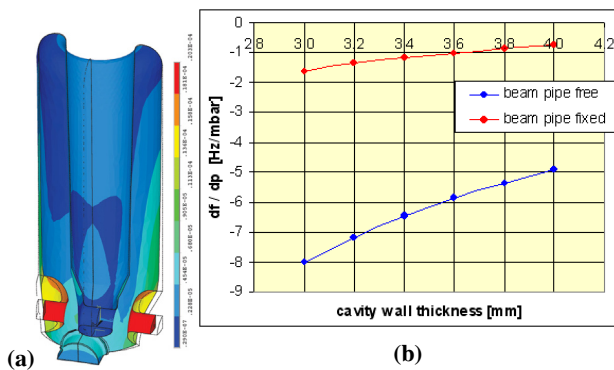


Figure 9: Structural analyses results of HWR with beam pipes free/fixed (a – cavity deformation).

Since the central part of cavity central electrode has been designed to maximize the stability of this part, the main frequency shift is caused by the beam port displacements. In this case the cavity has been simulated without helium vessel. The helium vessel adds rigidity to the beam ports and is equivalent approximately to the fully constrained conditions (Fig.10).

For simulations the helium vessel wall thickness 2 mm was used, the cavity walls were 4 mm except of central electrode walls with 3 mm. The cavity is jointed with helium vessel at beam ports, coupler port, tuner port and vacuum ports. There are no any constrains on all ports. There is a fixation of the he vessel model imitating the whole structure support in cryomodule.

An additional stiffening of the central part of the central electrode eliminates nearly all the cavity frequency dependence on external pressure (Fig.11). The cavity frequency dependence on external pressure that is close to zero in this case is explained not by an extreme low cavity deformations but by well-known effect of the self-compensation of frequency shifts caused by the change of

the volume occupied by the magnetic and electrical fields (described for instance in [5]). Fixation of ports causes only the minor change of the results.

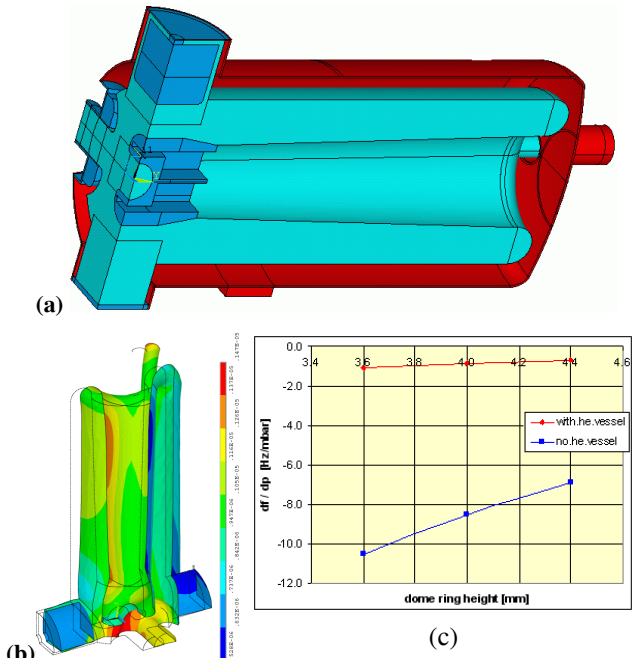


Figure 10: Coupled analyses model (a) and results (c) for HWR with and without He vessel (for cavity deformations (b) He vessel is not shown).

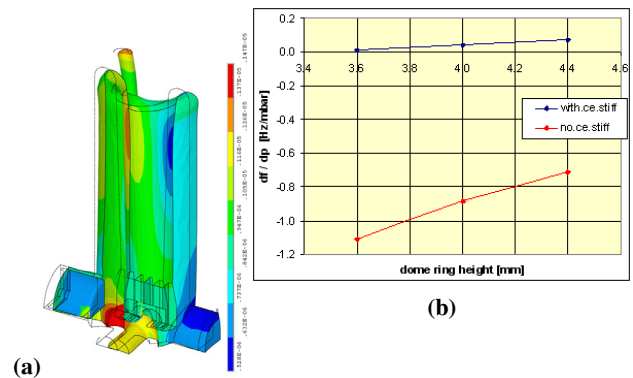


Figure 11: Structural analyses results of HWR in he vessel with and without central electrode stiffening (for cavity deformations (a) He vessel is not shown).

Modal Analysis

The structural modal analysis has been provided with helium vessel fixed at the supports and tuner fixed by the tuner stem. The results are summarized in Table 2.

Table 2: Mechanical modal analysis results of half-wave resonator in helium vessel.

	mode	1	2	3
modal analysis	Freq / Hz	136.32	160.95	234.14
prestressed modal analysis	Freq / Hz	136.95	161.98	234.75

The first eigen mechanical mode of the system “cavity in helium vessel” is related to the central electrode oscillation (Fig.12). Constrains of the model for these simulations are very arbitrary - vacuum ports are not constrained at all, the coupler port is simulated rather preliminary and is not constrained, too. The connection of the cavity with the helium vessel at the dome region is made through the joints at the ends of vacuum ports. Because of these differences from the real structure the first mechanical mode frequency is expected higher. To increase more this mode frequency the cavity should be connected with helium vessel at the cavity dome region.

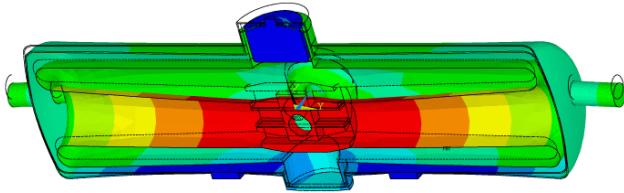


Figure 12: Cavity first eigen mechanical mode.

The same modal analyses on prestressed model (the modal under 1 bar external pressure) revealed no big difference of results (Table 3).

Static Lorentz Force Detuning

The measure of the static Lorentz force cavity detuning is a structure frequency shift relative to the accelerating cavity field square ($K_L = \Delta f / E_{acc}^2$). The action of the Lorentz forces in the region of the magnetic field is directed outwards and in the electric field region inward the cavity volume.

Lorentz force detuning is a function of RF field, which is forcing term, mechanical mode frequency, modal mass and mode’s damping degree. However, findings of mode frequencies, corresponding stiffness and especially damping degrees are quite difficult for the real situation, since these dynamic properties are very sensitive to the boundary conditions such as connection scheme, strength, equivalent masses and equivalent stiffness of surroundings that is attached to the cavity. Only the relative comparisons are available before having experimental measurements of mechanical properties with actual cryomodule. Even after having measured values about dynamic mechanical properties of cavity, the predictions are not accurate with a conventional RF modelling, since RF fields and mechanical vibrations are strongly coupled and both are dynamic.

LFD measurements can even differ much from one measurement to another since they are most sensitive to the cavity constrains in the cryostat. Additionally, the cavity displacements caused by Lorentz forces are within μm 's, and the cavity manufacture tolerances usually 100-200 μm . That’s why one should expect here the biggest difference between simulation and experimental data. The cavity constrains in the cryostat should be simulated as close to the reality as possible since they can play the dominant role for accuracy of the simulation results.

07 Cavity design

The response of HWR to a Lorentz force pressure was simulated. The numerical coupled analyses for Lorentz force detuning effect has been provided. An initial simulation of the cavity under different cryomodule environmental constrains can be made with two extreme cases – with completely free and fixed cavity components that are the joints with external structure. In our case they are beam pipes, vacuum ports, the coupler port and the tuner. The results of calculations for different joint conditions are presented in Table 3. The results can differ nearly two times, but the general conclusion that the cavity is rigid enough can be made.

Table 3: Lorentz force simulation results.

cavity wall = 4 mm	K_L Hz/(MV/m) ²
all free but LHe vessel support	-1.56
beam pipe fixed	-0.83
coupler flange fixed	-1.52
tuner fixed	-1.07

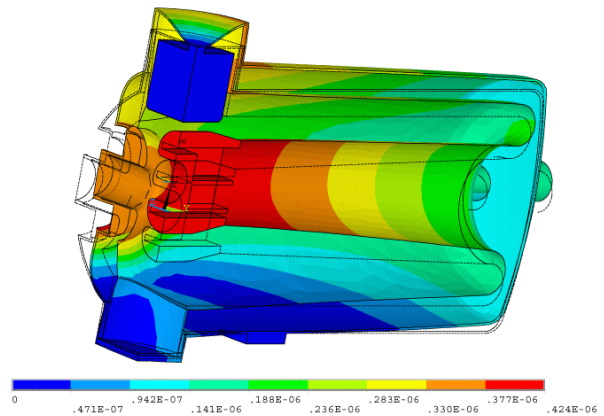


Figure 13: Cavity deformation under Lorentz force pressure.

ACKNOWLEDGEMENTS

We are deeply thankful to G. Romanov (FNAL) for many helpful explanations on multipactor simulations.

REFERENCES

- [1] A. Mosnier, „Development of IFMIF/EVEDA Accelerator“, PAC09, Vancouver, Canada, 2009.
- [2] E. Zaplatin et al, “IFMIF Superconducting $\beta=0.094$ Half-Wave Resonator Design”, PAC09, Vancouver, Canada, 2009.
- [3] G. Romanov, “Simulation of Multipacting in HINS Accelerating Structures with CST Particle Studio”, LINAC2006, Knoxville, USA, 2006.
- [4] E. Zaplatin, "FZJ SC Cavity Coupled Analyses" SRF2005, Ithaca, USA, 2005.
- [5] E. Zaplatin et al, "HIPPI Triple-Spoke Cavity Design", EPAC2006, Edinburgh, UK, 2006.